MECHATRONIC DESIGN OF A LOW TSR VERTICAL AXIS WIND TURBINE WITH VARIABLE PITCH ANGLE

Diego Alejandro Godoy Diaz
Fernando Augusto de Noronha Castro Pinto
Av. Horácio Macedo 2030 Centro de Tecnologia Bloco I-130
dgodoy@ufrj.br
fcpinto@ufrj.br

Abstract. *In this paper a mechatronic conceptual design of a low TSR vertical axis wind turbine with variable pitch angle is presented. The vertical axis wind turbine designed has three flat blades, high solidity for low wind velocities and its aerodynamic behavior is performed using a simplified multiple streamtube model. A small scale prototype was developed and it is operated by two Arduino boards, which are responsible for computing the implemented model and for controlling the pitch angle of each blade. It was used a permanent magnet stepper motor as actuator for each blade, and a two-axis Hall effect sensor to measure each blade pitch angle. Another Hall effect sensor is used for measuring the azimuthal angle of the rotor. It was established a communication protocol between each board and a computer as an observer by the author using the serial ports and two Bluetooth modules.*

Keywords: *Vertical Axis Wind Turbines, Wind Energy, Mechatronic Design, Variable Pitch Angle.*

1. INTRODUCTION

Harnessing of wind by human is not a recent technology, but the need to reduce the increasing consumption of fossil fuels in the last decades of the twentieth century led the dependent countries, mostly developed, to seek sustainable alternatives. Vertical axis wind turbines are still under research and improvements due to their lower efficiency compared with horizontal axis wind turbines. However, vertical axis Wind turbines could be an interesting low-cost solution in urban and residential areas, where investments in installation and maintenance would be lower than the common horizontal axis wind turbines.

It was developed a conceptual design of a vertical axis wind turbine (VAWT) with active linear control that adjust automatically its pitch angle of blades in order to improve the efficiency. A small scale prototype was build and first field tests were made.

2. VERTICAL AXIS WIND TURBINES

Wind turbines are classified in two principal groups depending of their rotation shaft. Most common are horizontal axis wind turbines (HAWT), due their higher efficiency than vertical axis wind turbines (VAWT) in large scales. A schematic representation of a typical HAWT and VAWT is shown in Fig. 1. The main difference between VAWT´s and HAWT behavior is that in VAWT the angle of attack varies in all the shaft rotation. Thus, HAWT angle of attack can be kept constant easier.

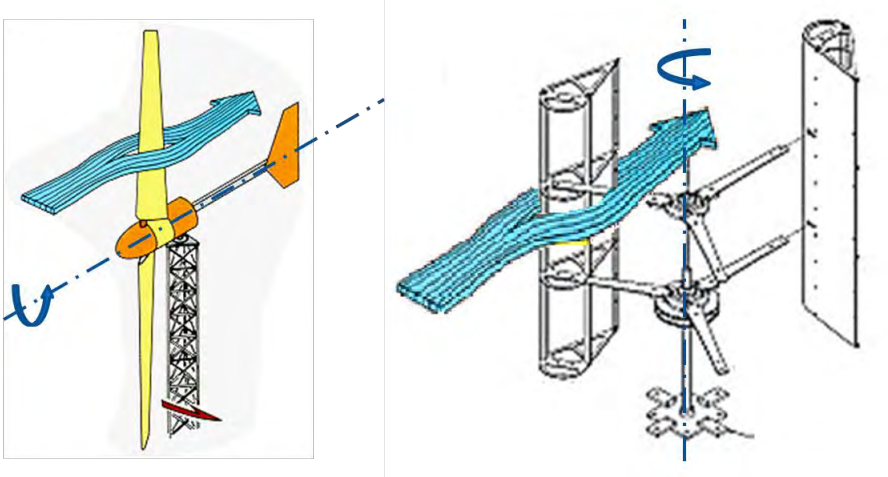

Figure 1. Horizontal Axis Wind Turbine (left) and Vertical Axis Wind Turbine (right)

Two important parameters of VAWT are the solidity (σ) and Tip Speed Ratio (TSR), expressed respectively as:

$$= \frac{Nc}{R} \tag{1}$$

$$TSR = \frac{\omega R}{V} \tag{2}$$

Solidity can be defined as the ratio between the total blade area and the projected turbine area (Tullis *et. al.*, 2011) where N is the number of blades, c the length of the chord, and the rotor radio R. TSR can be defined as ratio between the product of angular velocity of central shaft ω and the rotor radio, and wind velocity V. High solidity with low TSR means low efficiencies, but it could be improved adjusting each pitch angle of rotor.

2.1 Aerodynamic simplified model for Low TSR

A simplified model of turbine behavior was developed (Diaz and Pinto, 2011) based in Glauert's blade element theory (Glauert, 1948). Diagram of velocities and forces is shown in Fig. 2.

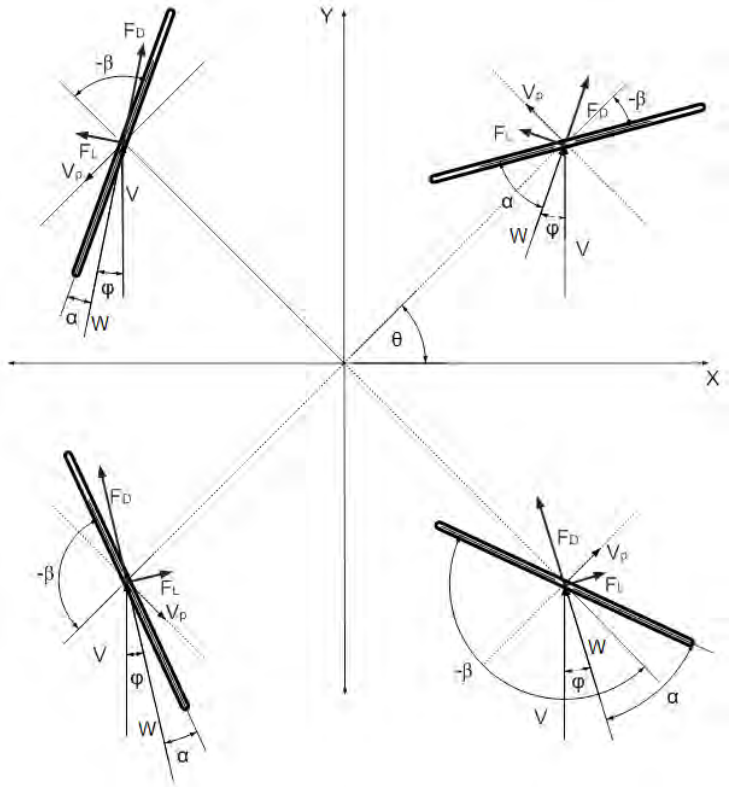

Figure 2. Top view of VAWT velocities and forces (Diaz and Pinto, 2011)

F_D and F_L are drag and lift forces respectively, W is the relative velocity between the linear blade velocity ($V_P = \omega R$) and the wind velocity V. θ is the azimuthal angle, α is the angle of attack, and β represents the pitch angle.

Using a simplified algorithm it was possible to compute the optimal angles, where it is produced the highest torque by the wind turbine.

This model approaches reasonably the aerodynamic behavior of high solidity rotors if $TSR < 1$, and in that condition it can be neglected the velocity losses downwind the rotor.

2.2 Applications of simplified model

An application of this model is the novel low tip speed ratio rotor developed at University of Wollongong, Australia (Cooper and Kennedy, 2011). This rotor has a passive mechanical control of the wind direction (yaw) and pitch angle of each blade, using a set of bevel gears with ratio 1:2, namely blade makes one revolution per two central shaft complete revolutions.

The most important advantage of this kind of turbine is the high starting torque that let the turbine rotate without the need of high wind velocities. In the other hand, the efficiency is lower than common wind turbines.

Figure 3 shows the schematic design of Wollongong's University vertical axis turbine. Using the algorithm proposed previously by author, optimal angles for several Tip Speed Ratios of a flat blade rotor are shown in Fig.4.

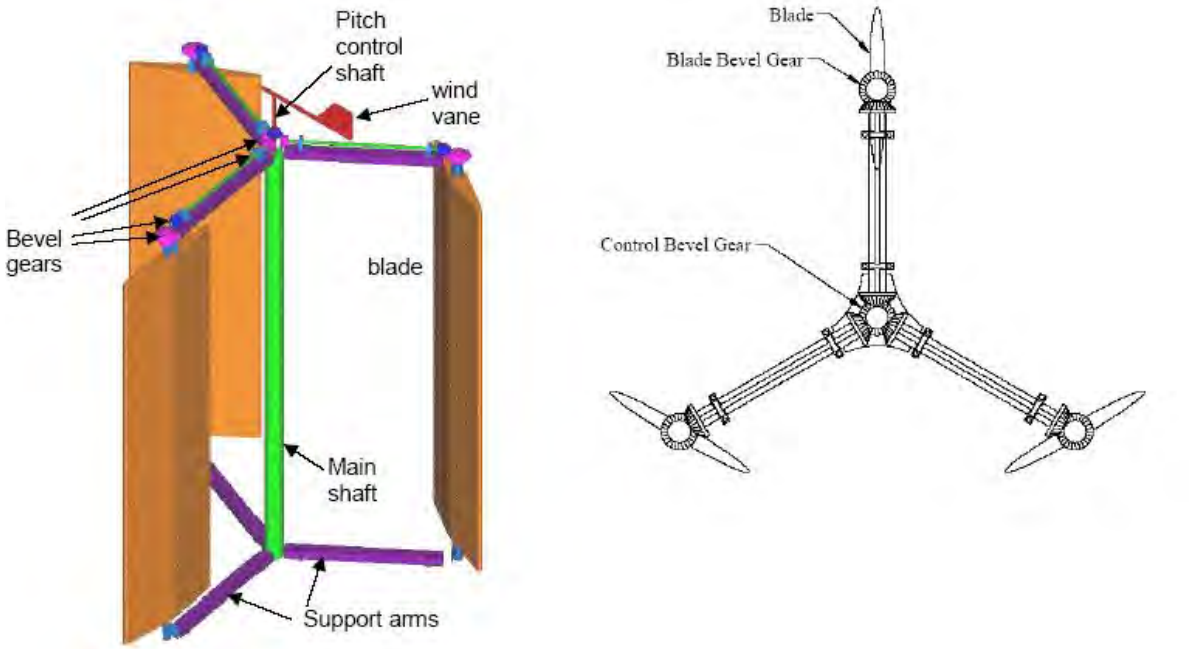

Figure 3. Wollongong University VAWT schematic design (Cooper and Kennedy,2011)

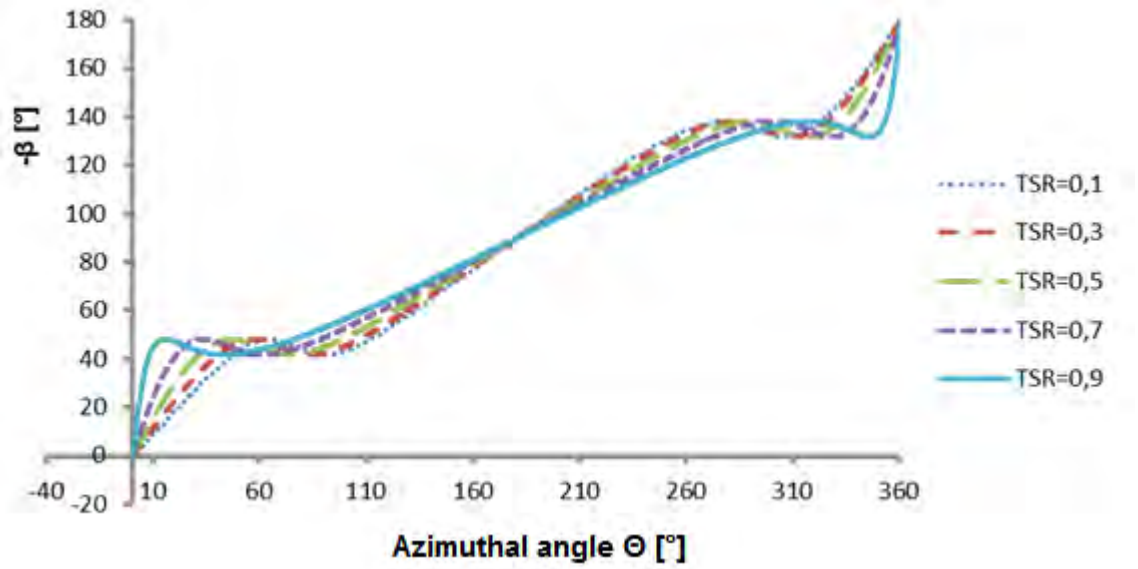

Figure 4. Optimal angles in each blade for some Tip Speed Ratios (Diaz and Pinto,2011)

A kind of four blade vertical axis wind turbine with active control of pitch angle was developed in 2006 (Seong *et. al*, 2006) using a servomotor for each blade as actuator. According to experimental data obtained by Seong, the turbine reached a reasonably efficiency (25% at $TSR = 2.2$), which means that blade linear velocity exceeded wind velocity, increasing its efficiency, a typical behavior of lift devices. Prototype and conceptual design developed by Seong *et. al.* are shown in Fig. 5.

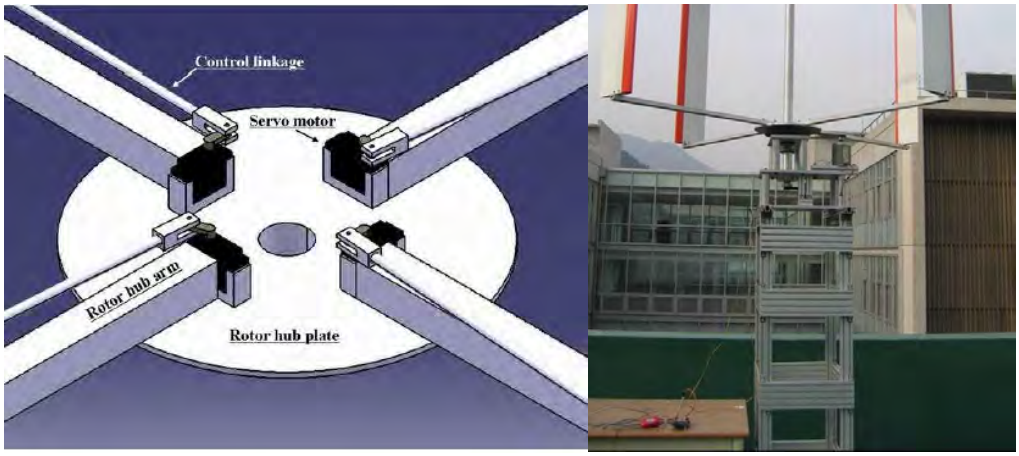

Figure 5. Four blade VAWT with active pitch control (Seong *et. al*,2006)

3. CONCEPTUAL DESIGN OF LOW TSR VAWT

The first feature to take into account for VAWT conceptual design was the operating principle of the rotor. In this case, the aim was develop a small low wind speed prototype ($V < 1\ m/s$). Because the rotor operates at low TSR, it needs high starting torques, so drag devices are more convenient in this case. One cheap and interesting solution is to use flat blades, due to their symmetry and easy fabrication. In this case, prototype was built with three flat blades.

The turbine mechanism developed was divided in two principal components: The first named as "Central Computing", which is responsible for measuring the azimuthal and yaw angle, computing the set point angles (optimal pitch angles) and sending via Bluetooth to the second one component, embedded into the rotor, called as "controller". This last component is responsible for measuring current blade pitch angles and computing the number of steps to reach the set point of each blade. PC is only connected for observation and visualization of transmitted data. Figure 6 shows an operating block diagram of developed VAWT. Communication between Central Computing and Controller is in a loop function, and it has protocols established by authors in order to guarantee the correct sending/receiving data.

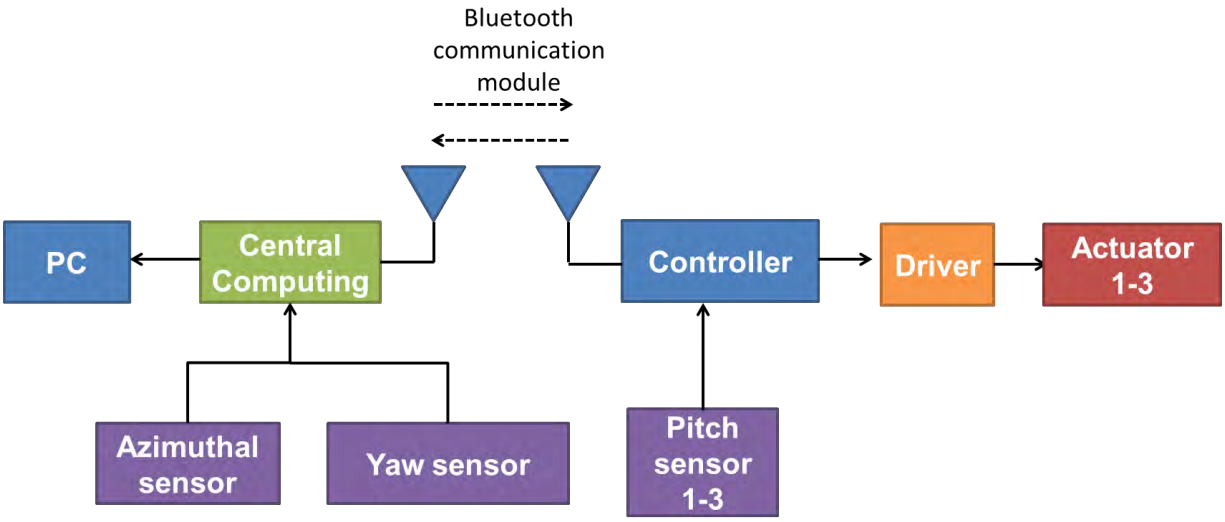

Figure 6. VAWTs operating Block diagram

Controller component is rotating with the rotor when operation of VAWT begins, powered by AA batteries. As a load, it was used a small DC motor. Central Computing is standing in external supports of VAWT. Figure 7 shows a conceptual design of developed VAWT. Figure 8 shows the prototype developed by the authors.

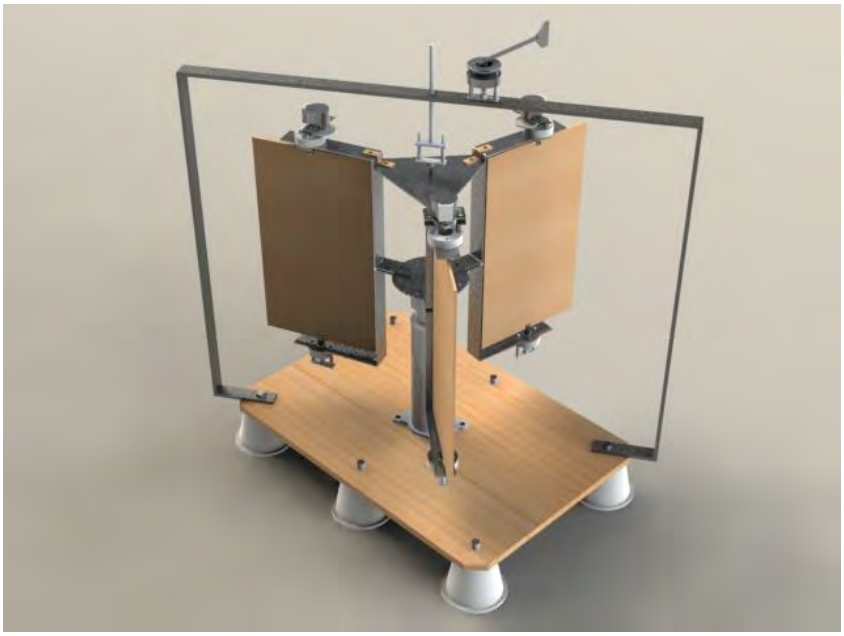

Figure 7. Conceptual design of vertical axis wind turbine

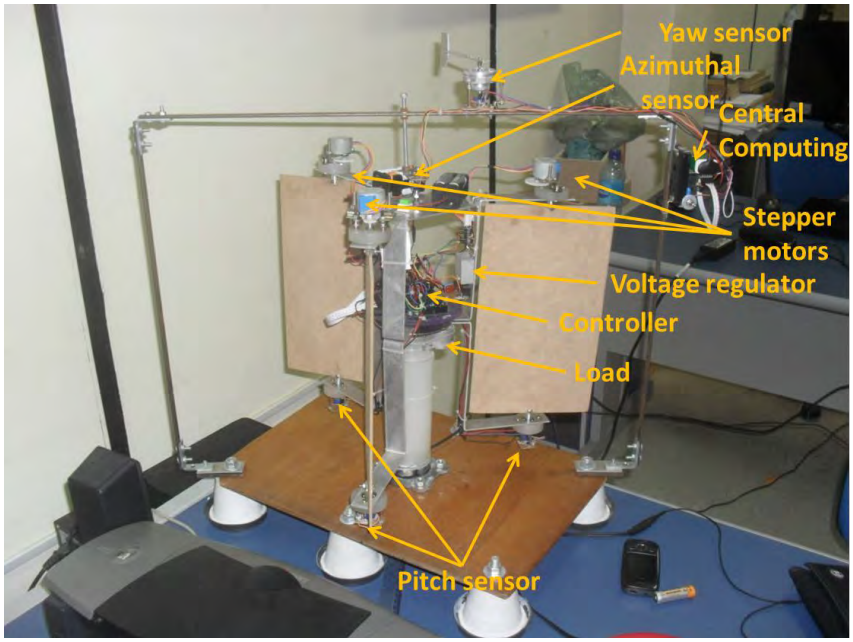

Figure 8. VAWT prototype developed

Parameters of prototype build are shown in Tab.1.

Table 1. Principal parameters of vertical axis wind turbine conceptual design

Parameters	Value
Height (m)	0,3
Radio (m)	0,17
Chord Length (m)	0,15
Number of blades	3
Airfoil reference	Flat blade
Blade Geometry	Straight

3.1 Angle sensors

Contactless absolute sensors were used in the VAWT prototype and they work with Hall's principles. The sensor is composed in a permanent magnet rotating around two Hall-effect axis sensor that produces a variation of magnetic fields lines, as shown in Fig. 9. With lines of magnetic fields changing, it is possible to obtain a correlation between sensor output voltage and the angle of the permanent magnet.

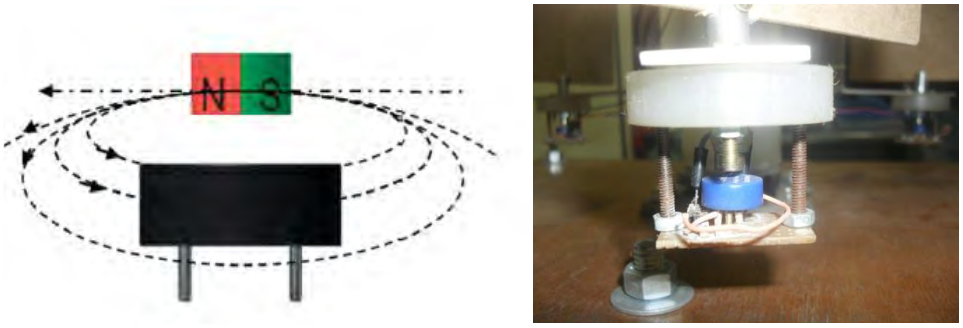

Figure 9. GMW360ASM Sensor principle diagram (left) and angle sensor mounted on prototype (right)

Sensor manufacturer provides a correlation between rotation angle and sensor output voltage (GMW, 2010), shown in Fig. 10, and it can be expressed as:

$$\beta = 90Vsensor - 225 \tag{3}$$

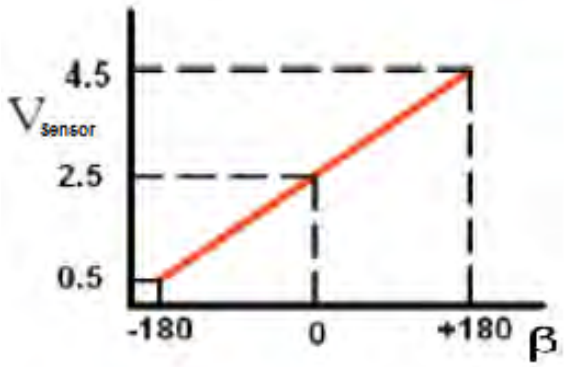

Figure 10. Correlation between rotation angle and sensor output voltage (GMW, 2010)

3.2 Actuators

As actuator, it was used permanent magnet stepper motors (28BYJ-5V), operating at 5V. Figure 11 shows the stepper motor linked to the blade shaft by two simple gear system. Power consumption of each motor is 1W.

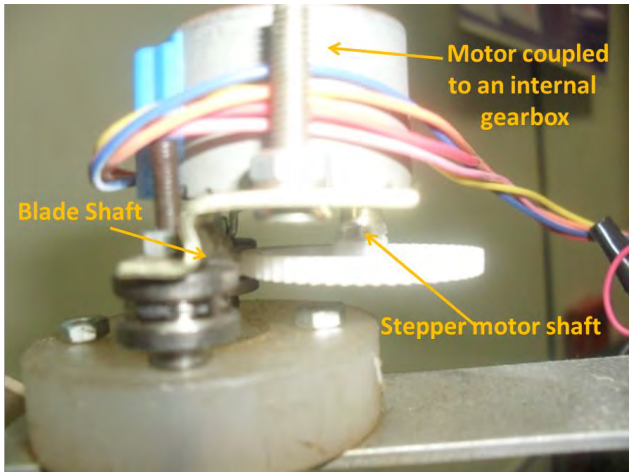

Figure 11. Stepper motor mounted on VAWT prototype

The operating principle of this type of motor is based on attraction forces generated by stator's induced current, which generates a polarity, thus a magnetic force that attracts the nearest opposite rotating pole (Fig. 12). Control component dedicates two digital outputs S1 and S2 for each actuator, in order to let rotate each stepper motor. The sequence of clockwise rotation is given by A + B + A-B + B + A-A +, and counterclockwise is B-A-B + A + B-A-A + B-, as shown in Tab 2.

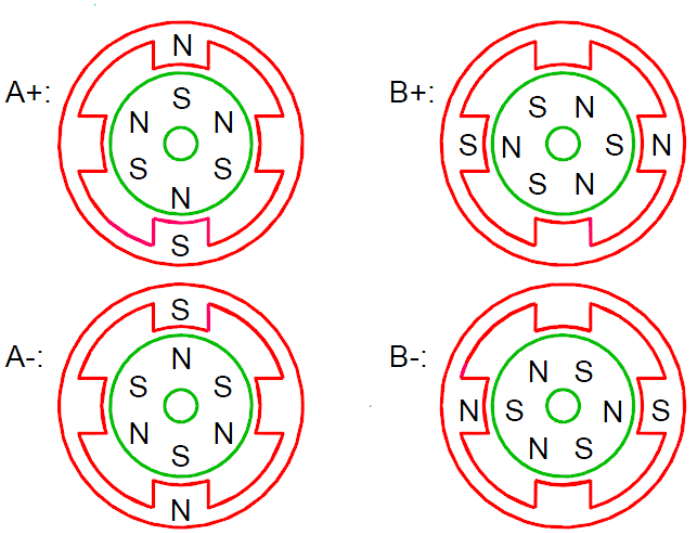

Figure 12. Rotating principle of permanent magnet stepper motor with 4 phases (Grimbledy, 2009)

Table 2. Sequence of stepper motor clockwise rotation

S1	S2	A+	B+	A-	B-
0	**0**	1	0	0	0
0	**1**	0	1	0	0
1	**0**	0	0	1	0
1	**1**	0	0	0	1

According to the manufacturer's datasheet of stepper motor used in prototype, the motor shaft is coupled to an internal gearbox whose ratio is 1:64, this means that for each revolution, the output gear of motor rotates 5.625 °. For this motor, a complete revolution in engine needs 8 steps, thus each sequence rotates the output gear 0,703 °.

For the torque transmission from stepper motor to blade shaft, it was necessary to couple two gears, whose teeth ratio ϑ defined as relation between motor shaft number of teeth and blade shaft gear number of teeth, and it can be expressed as:

$$\vartheta = \frac{Z_{motor}}{Z_{blade}} = \frac{55}{18} \cong 3{,}055 \tag{4}$$

Finally it can be established the number of motor steps per each degree of blade shaft rotation:

$$K = (\vartheta * 0{,}703°)^{-1} \cong 0{,}4655 \left[\frac{steps}{degrees}\right] \tag{5}$$

This means that for each motor step blade shaft rotates 2,148 degrees. The block diagram of blades controlling system is shown in Fig.13, where $K$is the linear transfer function which makes the equivalence between the error angle value and the number of steps (Eq. 5), βt is the transfer function involving sensor's voltage output and current pitch angle of each blade (Eq. 3). In this case, for first tests, these blocks have only proportional gain, neglecting the sensors dynamic response delay. For computation, pitch angle values are approximate to integer format. Because steps and degrees ratio are not synchronized (Eq. 5 is not equal to the unity), controller block permits a tolerance of ±4 degrees, in order to avoid problems with error convergence value when current pitch angle approaches the setpoint value.

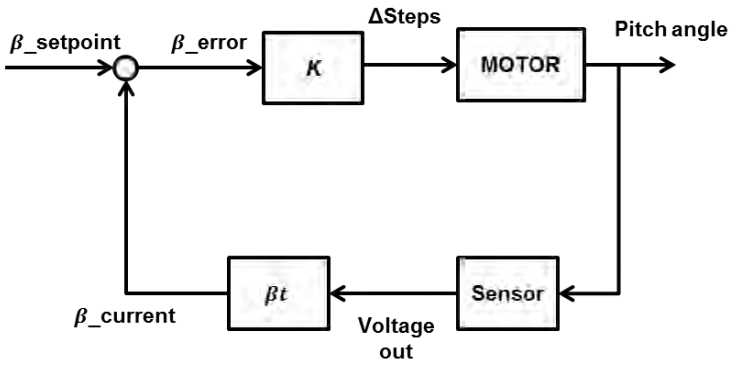

Figure 13. Blade control simplified blocks diagram (system has an angle tolerance of ±4 degrees).

3.3 Central computing and Controller components

The Central computing block is the responsible of measuring yaw and azimuthal angles, computing optimal pitch angles and sending the respective data to controller component. When data is sent, the Central computing block enters in standby state, and waits to receive the data package confirmation (with the string control defined by authors). Then elapsed time is measured and Central computing block algorithm start again, as shown in Fig. 14. Algorithm is implemented in an Arduino® Nano board.

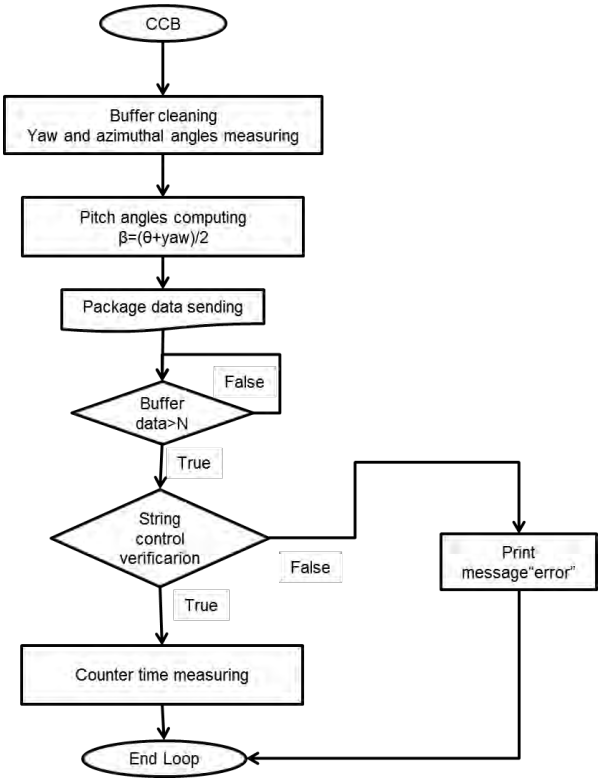

Figure 14. Flowchart of Central Computing Block (CCB) loop algorithm

Controller component receives the data package from the Central computing block, and evaluates the control strings in order to verify the correct data sending. In this block, there are two control verifications due to measured time data variation. When elapsed time is greater, more number of bytes is needed to represent that time value, then package size increases and an auxiliary string control is required. Figure 15 shows the Controller block logical algorithm flowchart, that was implemented in an Arduino® UNO board.

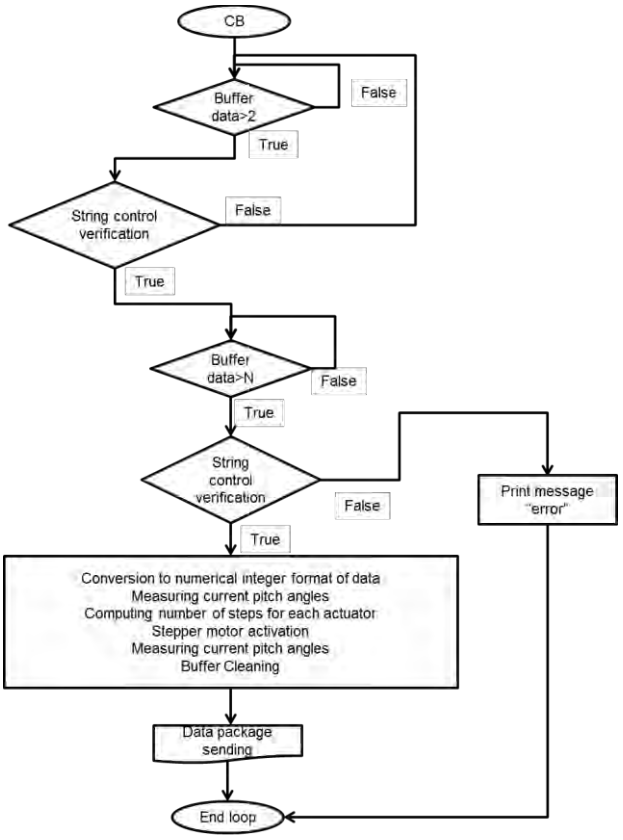

Figure 15. Flowchart of Controller Block (CB) loop algorithm

3.4 Communication

Communication between Central computing block and Controller block is established by simplified protocol, using some control strings in order to verify the correct send/receive process. Data are sent and received by a package of ASCII values, and internal algorithm functions permits convert their into integer format to compute the respective angle operations.

Data is transferred via serial at rate of 115,2 kbps, using a Bluetooth module in each block. Because time data varies in elapsed time, it is necessary use two data controls in the Central Computing block. Table 3 shows the order of data sent/received between Central Computing block and Controller Block.

Table 3. Data sent/received between Central Computing Block and Controller Block

CCB→CB	CB→CCB
Yaw angle	Current first blade pitch angle
Azimuthal angle	Current second blade pitch angle
Previous first blade pitch angle	Current third blade pitch angle
Previous second blade pitch angle	Control Data 1
Previous third blade pitch angle	
Elapsed time	
Control data 1 (2 ASCII strings)	
Set point of first pitch angle	
Set point of second pitch angle	
Set point of third pitch angle	
Control Data 2	

4. FIRST VAWT PROTOTYPE TEST

An experiment was conducted with a wind speed average $V = 0{,}9\ m/s$ to observe the prototype behavior. This experiment was performed with a fan of 0.5m rotor diameter at a distance d form the wind prototype, as shown in Fig. 16 (left). Yaw angle was kept fixed and the distance was established so that the wind could cover all the VAWT swept

area. To obtain this configuration, it was measured several regions with an anemometer, dividing the frontal projection of prototype in nine partitions as shown in Fig. 16 (right). With d=1.5m was obtained the most homogenous average speed in all nine partitions.

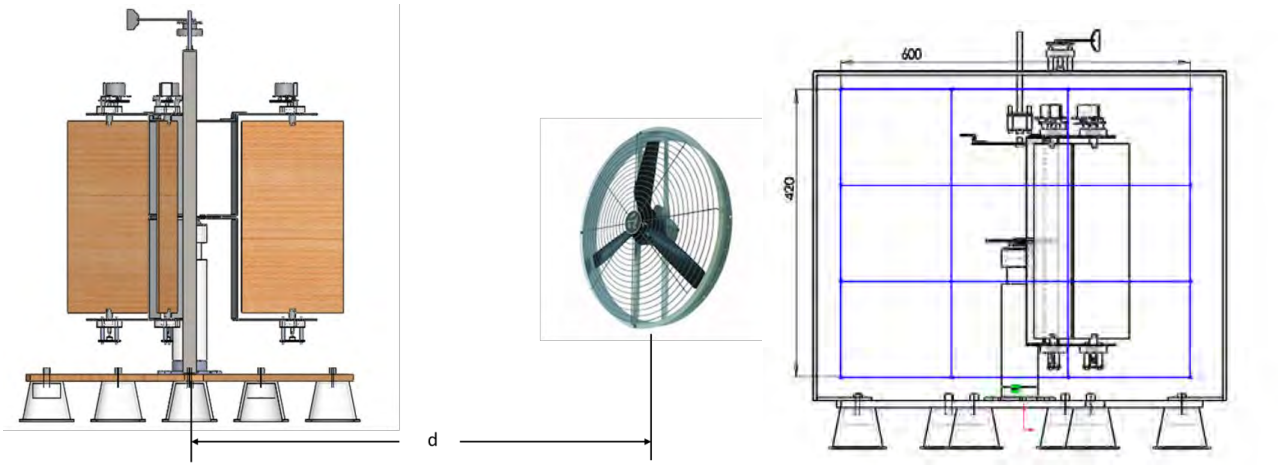

Figure 16. Configuration for first VAWT prototype test (left). Frontal projection in 9 partitions (right).

Experimental prototype velocity was obtained during 90 seconds of VAWT´s operation. Note that velocity tends to converge into a constant value (19 rpm) lower than average wind velocity source, as shown in Fig. 17. Using the Eq. 2, the tip speed ratio for this case is $TSR \cong 0{,}39$, being common in low tip speed ratios vertical axis wind turbines behavior.

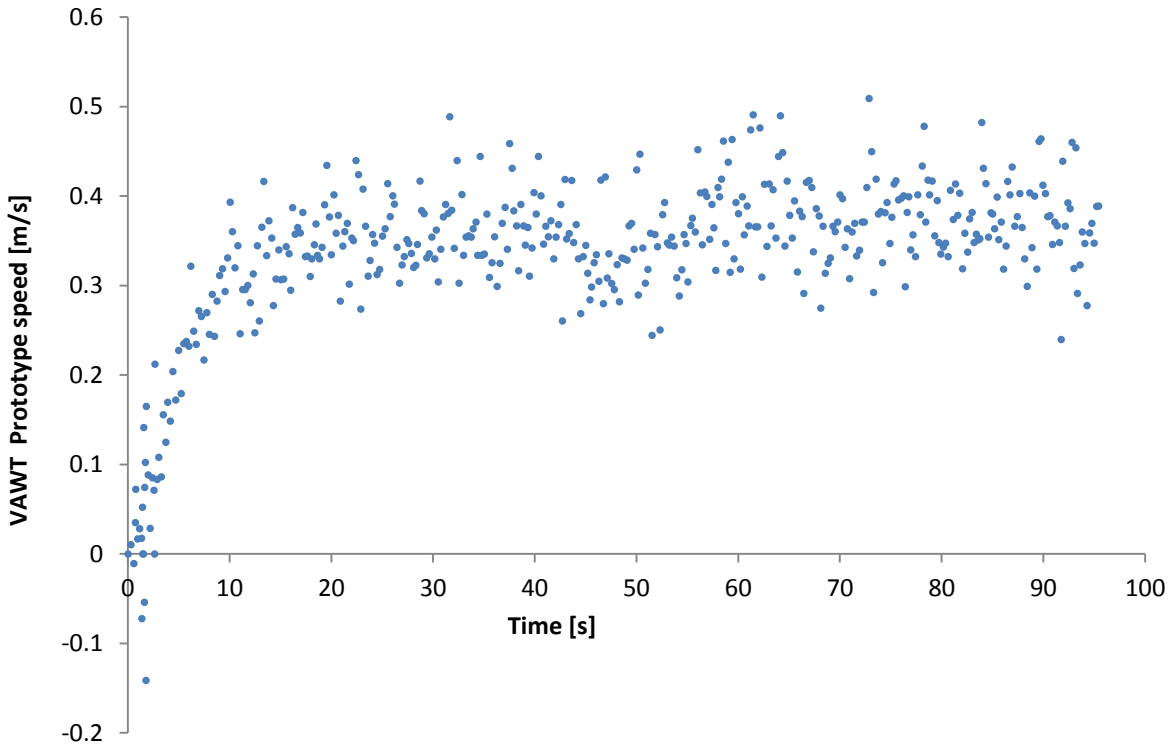

Figure 17. Velocity of VAWT prototype in function of time (95 seg)

Experimental pitch angles were obtained and plotted in function of azimuthal turbine angle, as shown in Fig. 18. It can be noted that simplified implemented model into Computer Computing Block is linear in first test, meaning that rotation ratio between turbine shaft and blade shaft is 2:1. It can be observed some dispersion on experimental measures. However, there is a tendency to follow the set point of all three pitch angles.

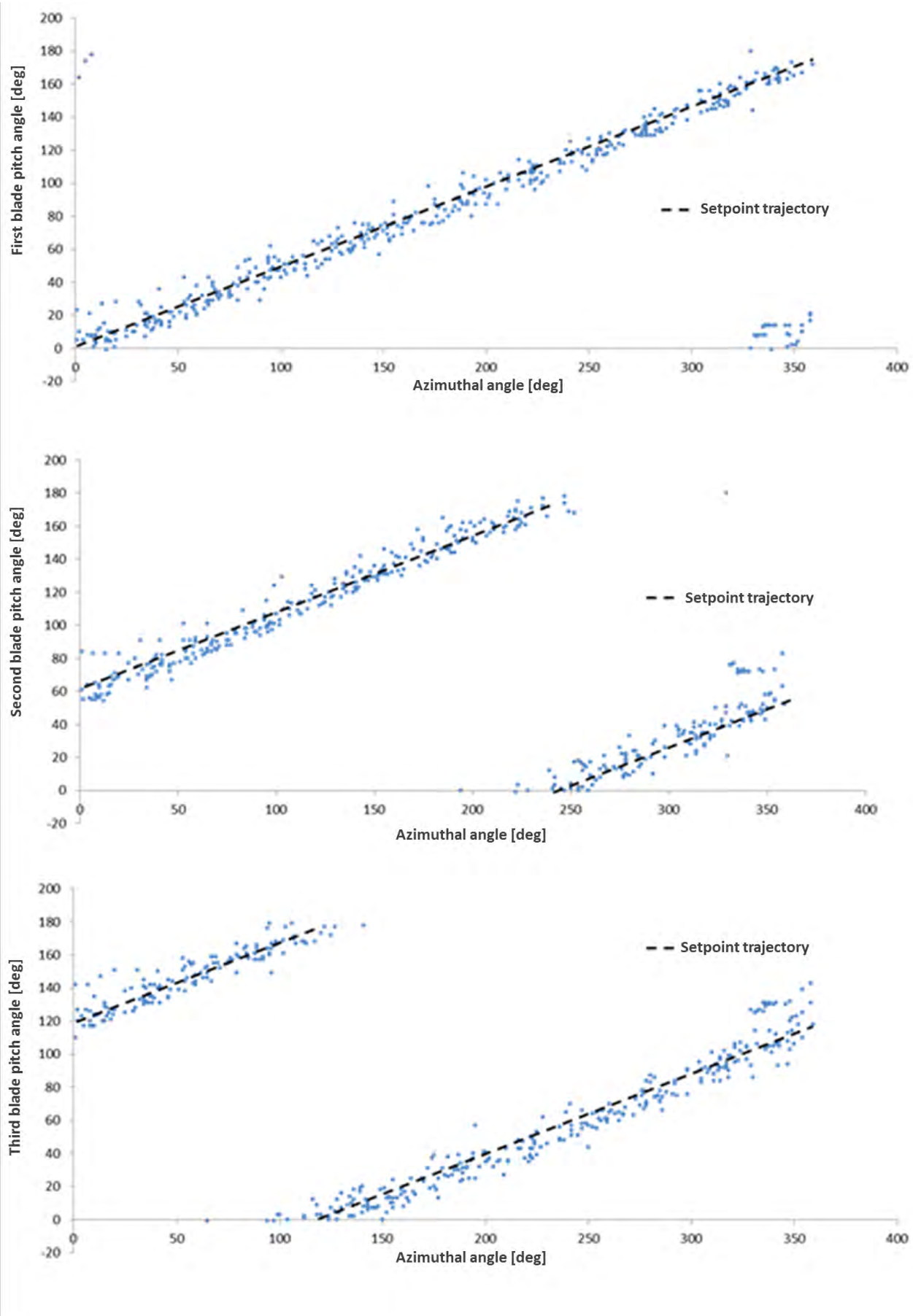

Figure 18. Pitch angles of the three blades in function of azimuthal turbine angle.

5. CONCLUSIONS

First test shows the evaluation of prototype behavior using a conventional fan as a wind source. Because wind regime is not controlled, induced velocities in the blades are not uniform, so first tests shows the prototype operating under turbulent conditions. It could be an interesting application for low heights VAWTs that works under drag forces principle. Futures tests will be made with more sophisticated wind sources, like wind tunnels.

There where dispersion in angles measuring, probably due to misalignment of the blade shaft and sensor axis, and turbulent regime of wind source. Another important reason could be the gears backslash of stepper motors mounted on the prototype, increasing the pitch angle tolerance. Nonetheless, experimental data shows a congruent behavior of expected results.

The aim of this work was study the behavior of controlled pitch VAWT angles, first with active control (requires external power), in order to synthesize a completely passive pitch control VAWT, more efficient and reliable than common low tip speed ratios VAWTs (i.e. Savonius rotor).

This first prototype will be subject to future improvements like more sophisticated and robust control, better aerodynamical blade geometry, in order to obtain more accurate experimental data.

6. REFERENCES

Cooper, P.; Kennedy, O., 2011. "Development and Analysis of a Novel Vertical Axis Wind Turbine". University of Wollongong. Wollongong, Australia.

Diaz, D. A.; Pinto, F. A. N., 2011. "Vertical Wind Turbine With Variable Blade Angular Position". *Proceedings of the 21st International Congress of Mechanical Engineering*. Natal, RN.

Glauert, H., 1947.The Elements Of Aerofoil and Airscrew Theory. 2. ed. Cambridge University Press. Cambridge, England.

Gmw. 2010, GMW360ASM Angle Sensor Module. GMW. San Carlos, USA. 10 Apr. 2012 <http://www.gmw.com/magnetic_sensors/sentron/2sa/GMW360ASM.html>.

Grimbledy, J.2009 Stepping Motors. University of Reading. Reading, England, 15 Apr. 2012, <http://www.personal.rdg.ac.uk/~stsgrimb/teaching/stepping_motors.pdf>.

Seong, I. et al. , 2006. "Efficiency improvement of a new vertical axis wind turbine by individual active control of blade motion". *SPIE Proceedings*. San Diego, USA: SPIE.

Tullis, S., Fiedler, A., McLaren, K., & Ziada, S., 2011. "Medium-solidity Vertical Axis Wind Turbines for use in Urban Environments". Hamilton, Canada.

7. RESPONSIBILITY NOTICE

The authors are the only responsible for the printed material included in this paper.